Different Conformational Changes within the F-Helix Occur during Serpin Folding, Polymerization, and Proteinase Inhibition†

Lisa D. Cabrita, Weiwen Dai, and Stephen P. Bottomley*

Department of Biochemistry and Molecular Biology, P.O. Box 13D, Monash University, Melbourne, Australia 3800

Received April 28, 2004; Revised Manuscript Received May 21, 2004

ABSTRACT: The intrinsic metastability of the serpin native state is the thermodynamic driving force for both proteinase inhibition and the formation of inactive polymers. A number of mechanisms has been proposed to explain how both these conformational changes are achieved. However, one aspect that has received little attention is the movement of the F-helix, which physically impedes both these events. We have applied a protein engineering approach to investigate the conformational changes of this helix during proteinase inhibition, serpin folding, and polymerization. We systematically mutated two highly conserved hydrophobic residues on the F-helix, V161 and I157, and in addition, removed a hydrogen bond between D149 and the first turn of the helix. Our data demonstrate that while all three interactions are important for the stability and folding of the molecule, their contribution during inhibition and polymerization differ. The presence of I157 is crucial to all conformational changes as its loss results in inactivation of the serpin and rapid polymerization. The replacement of D149 does not affect activity but significantly increases the polymerization rate. The interactions formed by V161 play an important role only in maintaining the native conformation. Taken together, these data suggest that the F-helix undergoes a reversible conformational change in both its N- and C-termini during proteinase inhibition only the C-terminus undergoes changes during polymerization, but there is a global change required for folding.

Members of the serine proteinase inhibitor (serpin) family have the inherent ability to undergo dramatic structural conversions (*1, 2*). These structural changes are essential for successful proteinase inhibition (*3, 4*); however, they also form the molecular basis for a range of devastating human diseases (*5, 6*). Understanding how these structural changes are accomplished is an intriguing problem with important implications in both biological and medical sciences. The native serpin molecule consists of three β-sheets (A−C) surrounded by nine α-helices (Figure 1A) (*7*). Extending from the fifth strand of the A β-sheet is the reactive center loop (RCL), which is the region that directly interacts with the proteinase. A large body of evidence has shown that the native serpin molecule is metastable and that it is only when the RCL is inserted into its own A β-sheet that the serpin adopts a thermodynamically more stable structure (*8, 9*). However, the fundamental cause behind an increasing number of diseases is that the RCL residues of one serpin can also insert into the A β-sheet of another serpin molecule, leading to the assembly of long polymers (Figure 1B) (*10, 11*). These polymers can deposit within tissues and cause diseases such as emphysema, liver cirrhosis, dementia, and thrombosis.

The structural change involved in both proteinase inhibition and serpin polymerization involves the insertion of RCL residues into the A β-sheet of either itself or another serpin molecule (Figure 1B). Analysis of the serpin architecture reveals that this is not a simple structural change as one element of secondary structure, the F-helix, forms a substantial barrier during both proteinase inhibition and serpin polymerization (Figure 1A,B) (*12*). Previously, is has been proposed that during inhibition, the A β sheet opens, in a shutter-like movement, with the F-helix moving as a block with strands 1−3 of the A β-sheet (*13*−*15*). However, the delta structure of α_1-antichymotrypsin revealed that the F-helix could unwind its C-terminus and insert these residues into the A β sheet (*16*). This conformational change was coupled with partial insertion of the RCL at the top of the A β-sheet, therefore suggesting that the F-helix can physically open up the A β-sheet to allow complete insertion of the RCL. The authors proposed that this conformation is formed during proteinase inhibition, serpin folding, and polymerization reactions.

We have recently shown that the F-helix is conformationally labile and capable of conformational change without significant structural change within the rest of the molecule (*17*). This instability is also supported by studies using antibodies that suggested that within the serpin−proteinase complex the F-helix is in equilibrium between a number of conformational states (*18, 19*). These and other data have lead to the hypothesis that a conformational change within the F-helix is essential during proteinase inhibition to overcome an energetic barrier. As such, the F-helix plays an "active, critical role" during proteinase inhibition (*12*).

In this work, we have taken a protein engineering approach to address the role of the F-helix in both proteinase inhibition and serpin polymerization using the α_1-antitrypsin (α_1-AT).[1]

† This work was supported by grants from the National Health and Medical Research Council and the Australian Research Council to S.P.B. S.P.B. is a Monash University Senior Logan Fellow and an R. D. Wright Fellow of the NHMRC.

* To whom correspondence should be addressed. Phone: 61-3-99053703. Fax: 61-3-99054699. E-mail: steve.bottomley@med.monash.edu.au.

[1] Abbreviations: α_1-AT, α_1-antitrypsin; SI, stoichiometry of inhibition.

10.1021/bi0491346 CCC: $27.50
Published on Web 07/10/2004

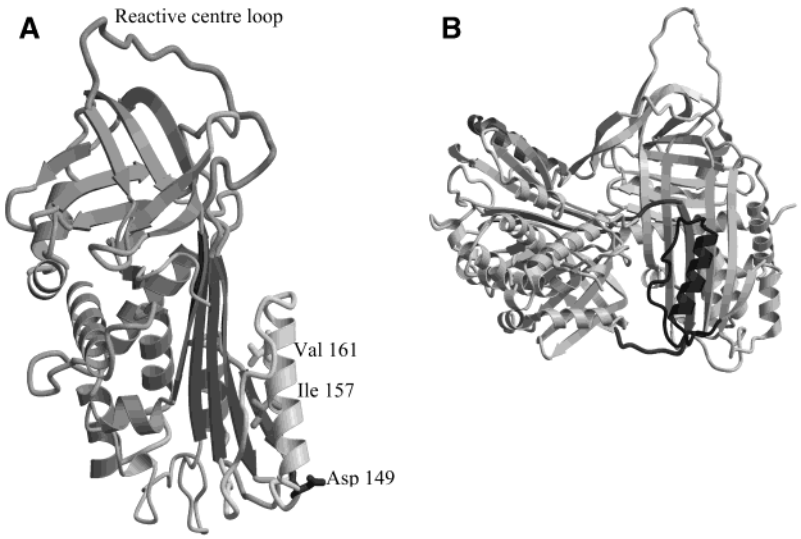

FIGURE 1: Schematic representation of native and polymerized α_1-AT. (A) Ribbon diagram of native α_1-AT with the reactive center loop and the side chains of V161, I157, and D149A highlighted. (B) Ribbon diagram of the dimer unit from polymerized α_1-AT; the F-helix of the acceptor molecule is shaded dark gray (*11*).

The F-helix lays across the A β-sheet and is comprised of four turns, a loop, and a hinge region adjoining the helix to strands 3A and 1A. The helix is anchored to the A β-sheet through a number of interactions. The most highly conserved residues on the F-helix are V161 and I157, which are conserved in over 70% of all serpin sequences (*20*). Both V161 and I157 form hydrophobic interactions with both the major loop of the F-helix as well as with strands 3A and 2A. To investigate the role of the F-helix in proteinase inhibition and polymerization, we investigated the contribution of both V161 and I157 to the inhibitory, folding, and misfolding reactions of α_1-AT. In addition, we investigated the contribution of a single hydrogen bond formed between D149 and the backbone of the first turn within the helix (Figure 1A). Through kinetic analysis of six variants, our data suggests that the F-helix undergoes a conformational change within both its N- and C-terminal regions during inhibition and folding, whereas only the C-terminal region deforms during serpin polymerization.

MATERIALS AND METHODS

Cloning, Mutagenesis, and Expression

To study the role of the residues V161, I157, and D149, we created seven variants proteins using α_1-AT as our template (*21*). V161 was mutated to an alanine, leucine, and isoleucine to produce the variants V161L, V161A, and V161I, respectively, while I157 was mutated to alanine, leucine, and valine to produce the variants I157A, I157L, and I157V. D149 was mutated to alanine to produce the variant D149A. All mutations were confirmed by DNA sequencing, and the proteins' identity was also confirmed by mass spectrometry. The proteins were expressed and purified as previously described (*21*).

Determination of the Stoichiometry of Inhibition and Rates of Inhibition

All kinetic measurements were performed in a buffer consisting of 50 mM Tris, 150 mM NaCl, 0.1% (w/v) PEG 8000, pH 7.4. Both the stoichiometry of inhibition (SI) and the association rate constant (k_{app}) between chymotrypsin and the α_1-AT variants were determined at 37 °C as previously described (*22*).

Thermal Denaturation

Thermal denaturation was performed on a Jasco 810 spectropolarimeter. The heating rate was 60 °C/h, and the change in the far-UV signal at 222 nm was monitored. The data were analyzed as previously described (*23*).

Chemical Denaturation

Stock solutions of guanidine hydrochloride (GdnHCl) in 50 mM Tris, 50 mM NaCl, 1 mM DTT (pH 7.8) were prepared and filtered through 0.22 μm membranes before use. The GdnHCl concentration was determined by refractive index measurements as previously described (*24*). Equilibrium unfolding curves were determined by measuring the CD signal at 222 nm as previously described (*21*).

Equilibrium Unfolding Analysis

All unfolding curves were found to be fully reversible, and the data were fit to a three-state unfolding model using a nonlinear least-squares fitting algorithm as described (*21*). The three-state analysis recognizes the presence of one stable intermediate structure (I), populated during the transition from the folded state (N) to the unfolded state (U). The changes in conformational stability for each mutant ($\Delta\Delta G$) were calculated using the following equation:

$$\Delta\Delta G = \langle m \rangle \Delta D_m \quad (1)$$

where ΔD_m is the difference between the value of ΔD_m for the wild-type−mutant protein, and $\langle m \rangle$ is the average m value (1.9 kcal/mol/M for the first transition and 0.72 kcal/mol/M for the second transition). This method is preferable as the m values varied between 1.7 and 2.1 kcal/mol/M, whereas the D_m was highly reproducible with standard deviations of 0.03 M.

Kinetics of Polymer Formation

Bis-ANS fluorescence measurements were all performed in 50 mm Tris, 1 mM DTT, 50 mM NaCl, pH 7.8. The

Table 1: Inhibitory and Thermal Stability Characteristics of Modified α_1-AT

	SI[a]	k_{app}[b] ($\times 10^6$ M^{-1} s^{-1})	k_{app}[c] ($\times 10^6$ M^{-1} s^{-1})	T_M (°C)
α_1-AT	1.1 ± 0.1	1.2	1.2	59 ± 0.5
D149A	1.1 ± 0.05	1.3	1.3	56 ± 1
I157L	1.7 ± 0.2	0.71	1.2	54 ± 1
I157V	1.8 ± 0.2	0.84	1.5	53 ± 1
V161A	1.1 ± 0.1	1.5	1.5	55 ± 1
V161I	1.1 ± 0.2	1.3	1.3	58 ± 1
V161L	1.2 ± 0.1	1.7	1.9	57 ± 0.5

[a] Stoichiometry of inhibition measured by titration of fixed amounts of chymotrypsin with α_1-AT or its variants as described in Materials and Methods. Average values ± SE from at least four titrations are reported. [b] Calculated using the total concentration of α_1-AT. [c] Calculated using the fractional concentration of α_1-AT that forms an inhibitory complex with chymotrypsin as described in the Materials and Methods.

fluorescence measurements were performed on a Perkin-Elmer LS50B spectrofluorimeter; a constant temperature was maintained with a thermostated cuvette holder and a circulating water bath. The solution in the cuvette (1 mL) was stirred constantly, and fluorescence data were recorded every 1 s. An excitation wavelength (λ_{ex}) of 410 nm was used, and the emission wavelength (λ_{em}) was 480 nm; excitation and emission slit widths were 5 nm. The reaction mixture was prewarmed to 60 °C, and the bis-ANS fluorescence signal was stabilized prior to addition of the protein. The polymerization kinetic data was characterized as previously described (*25*).

RESULTS AND DISCUSSION

To probe the structural changes within the F-helix during proteinase inhibition, serpin folding, and polymerization, we mutated the highly conserved residues V161 and I157, both of which form hydrophobic interactions with the A β-sheet, and also D149, which forms a hydrogen bond at the N-terminus of the helix (Figure 1). Seven variants, V161A, V161I, V161L, I157L, I157V, I157A, and D149A, were generated. Each variant was expressed in a soluble form and purified to homogeneity, with the exception of I157A, which could not be purified in a monomeric form and as a result was not studied further.

Effects of Mutation within the F-Helix upon the Stoichiometry of Inhibition and Rate of Inhibition

The SI data show that there is a clear distinction in the roles played by these three residues situated on the helix F (Table 1). Removal of the hydrophobic interactions between V161 and the A β-sheet and the hydrogen bond between D149 and the first turn of the F-helix have little effect on the serpins' functionality. All the variants at position 161 and 149 had SI values virtually indistinguishable from α_1-AT (Table 1). These data were confirmed by SDS−PAGE analysis of the reaction components, which showed only the presence of a serpin−proteinase complex (data not shown). In addition, the apparent second-order rate constants for inhibition (k_{app}) for all the V161 variants and D149A were similar to those of α_1-AT.

The replacement of I157 with either leucine or valine resulted in less efficient inhibitors, with SI values of 1.7 and 1.8 for I157L and I157V, respectively. The mutations also resulted in k_{app} values approximately 2-fold slower than α_1-AT (Table 1). However, when the k_{app} for the variants was corrected for their respective SI values, to produce k'_{app} (*26*, *27*), the values were comparable to α_1-AT (Table 1). These data indicate that the mutations affect the conformational changes occurring after docking of the proteinase (i.e., during translocation of the proteinase from one end of the serpin to the other). These data suggest that the interactions formed between I157 and the A β-sheet must be maintained throughout the inhibitory reaction, as their loss results in increased substrate behavior. In contrast, both the V161 variants and the D149A do not appear to affect the SI and k'_{app}, and as such, it would indicate that both the N- and the C-terminal portions of the helix undergo reversible deformation during inhibition, whereby these interactions are broken (Figure 4). Thus, conformational change occurring within both termini of the F-helix facilitates rapid proteinase translocation and inhibition.

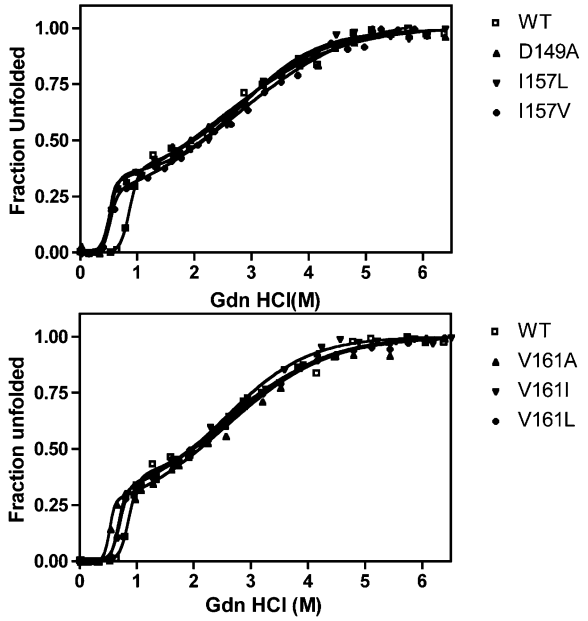

FIGURE 2: Unfolding of the F-helix variants. The far-UV CD signal at 222 nm is shown as a function of GdnHCl concentration for 0.2 μM protein in 50 mM Tris, 50 mM NaCl, 1mM DTT, pH 7.8 at 25 °C in a 1 mm cuvette.

Effects of Mutations within the F-Helix upon Serpin Stability

The thermal stability of each variant was measured using far-UV circular dichroism (Table 1). The thermal melts obtained for the V161 and D149 variants show that the mutations had a destabilizing effect on the serpin structure. The presence of alanine at both V161 (T_M = 55 ± 1 °C) and D149 (T_M = 56 ± 1 °C) destabilized the native state relative to α_1-AT. The presence of either leucine (T_M = 53 ± 1 °C) or valine (T_M = 54 ± 1 °C) at position 157 was more destabilizing, indicating that the interactions formed by I157 are important to maintenance of the native state.

GdnHCl unfolding of the variants was monitored using far-UV CD (Figure 2). The unfolding behavior of α_1-AT has been well-studied and shown to correspond to a reversible three-state process in which one intermediate species is populated under moderately denaturing conditions (*28*−*31*). All the variants displayed an N → I transition that occurred

Table 2: Effects of Mutations within the F-Helix on the Stability and Polymerization Kinetics of α_1-AT

	D_{NI}[a] (M)	$\Delta\Delta G_{NI}$[a] *(kcal mol)*	D_{IU}[a] (M)	$\Delta\Delta G_{IU}$[a] (kcal mol)	ϕ_I[b]	k_{cc}[c] (s^{-1})	k_{agg}[c] (s^{-1})
WT	0.85		2.50			0.025 ± 0.003	$4 \pm 0.1 \times 10\text{-}4$
D149A	0.49	−3.36	2.50	0.00	0	0.097 ± 0.005	$2 \pm 0.2 \times 10\text{-}3$
I157L	0.49	−3.36	2.55	0.03	0.01	0.24 ± 0.01	$3 \pm 0.1 \times 10\text{-}3$
I157V	0.53	−2.9	2.70	0.16	0.05	0.36 ± 0.03	$4 \pm 0.2 \times 10\text{-}3$
V161A	0.53	−2.9	2.64	0.09	0.03	0.11 ± 0.004	$6 \pm 0.2 \times 10\text{-}4$
V161I	0.71	−1.31	2.55	0.038	0.03	0.021 ± 0.004	$3 \pm 0.2 \times 10\text{-}4$
V161L	0.68	−1.6	2.4	−0.06	0.04	0.031 ± 0.003	$3 \pm 0.1 \times 10\text{-}4$

[a] The unfolding data from Figure 2 were analyzed using a three-state model as described in the Materials and Methods; the results represent the average of five individual unfolding curves. D_{NI} and D_{IU} represent the midpoint of denaturation for the native to intermediate and intermediate to unfolded transitions, respectively. $\Delta\Delta G_{NI}$ and $\Delta\Delta G_{IU}$ represent the difference in free energy between the variants and α_1-AT for the native to intermediate and intermediate to unfolded transitions. [b] ϕ_I is the integrity value of the interactions as described in the Results and calculated as previously described (*32*, *33*). [c] The kinetics of polymerization were determined by following the changes in bis-ANS fluorescence as previously described (*25*); each value represents the average of five independent time courses. k_{cc} represents the rate of conformational change, and k_{agg} represents the rate of aggregation.

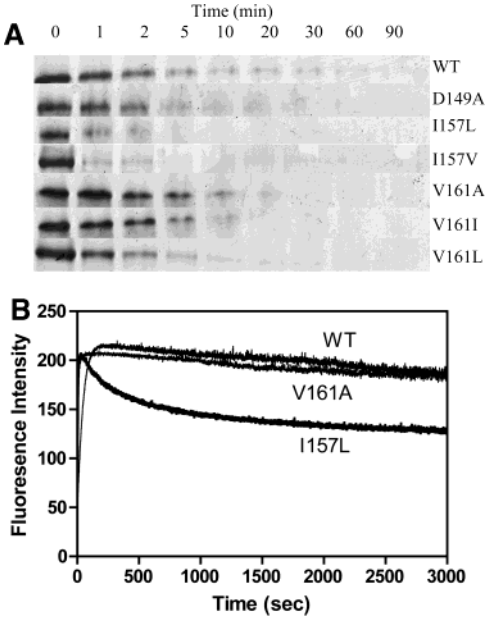

FIGURE 3: Characterization of the polymerization properties of the F-helix variants. (A) Samples of protein (10 μM) were incubated at 60 °C and then removed and analyzed by native-page at the time points indicated. The figure follows the loss of monomeric protein band with time. (B) The change in bis-ANS fluorescence was followed when the proteins (10 μM) were incubated, with constant stirring, at 60 °C in a 1 cm quartz cuvette.

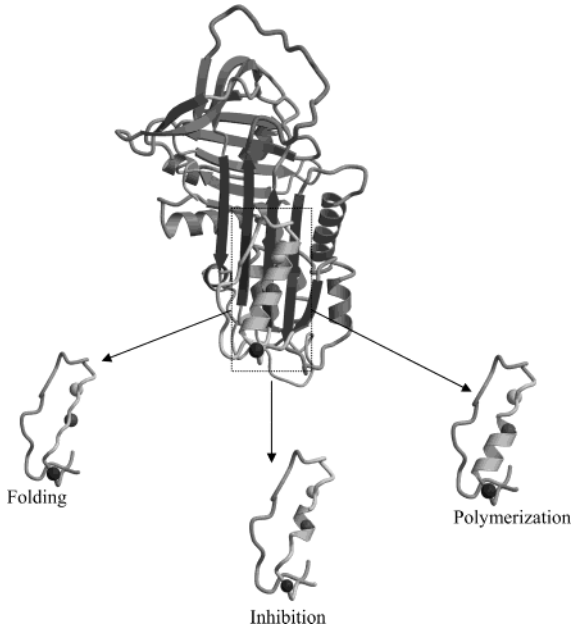

FIGURE 4: Schematic representation of F-helix movements. Top: ribbon diagram of α_1-AT with the F-helix highlighted. Bottom: schematic illustrating the alternative conformations of the F-helix during folding, inhibition, and polymerization. Regions that do not undergo structural change are represented by ribbons, and the region undergoing conformational change is shown as a coil.

up to 0.3 M GdnHCl lower than α_1-AT, indicating that the native state of the variants was destabilized by up to 3 kcal/mol. The mutations, however, had no effect upon the I → U transition (Figure 2 and Table 2). To determine the relative integrity of each interaction within the native and intermediate state, we used ϕ_I analysis. This analysis has been used by several groups to investigate the structure of equilibrium intermediates (*32*, *33*). The difference in free energy of unfolding between the wild-type protein and the mutant is calculated for both the native/intermediate ($\Delta\Delta G_{NI}$) and intermediate/unfolded ($\Delta\Delta G_{IU}$) transitions. The integrity of a given interaction within the intermediate ensemble (ϕ_I) is then given as

$$\phi_I = \Delta\Delta G_{IU}/\Delta\Delta G_{NU}$$

where $\Delta\Delta G_{NU} = \Delta\Delta G_{NI} + \Delta\Delta G_{IU}$. A ϕ_I close to 0 indicates that the interaction removed by mutation is lacking in the intermediate, and a ϕ_I of 1 indicates that the interaction is present in the intermediate. The ϕ_I values for all of the mutations were very close to 0 (Table 2), indicating that the interactions formed by these residues in the native state are not present in the intermediate. Therefore, the whole length of the F-helix is in a non-native conformation within the intermediate ensemble (Figure 4). Additionally, our data suggest that the conformation of the intermediate ensemble is not the δ structure (*16*), as both I157 and V161 form a significant number of interactions in this conformation.

Characterization of the F-Helix Mutations upon Polymerization

Serpin polymerization is the molecular basis for a wide number of disease states (*10*). α_1-AT forms polymers through a two-step process, in which the native protein forms a partially structured species (termed M*), which then self-associates to form long chain polymers (*34*, *35*). In this

process, the A β-sheet expands, allowing the insertion of the RCL from another molecule, and it is clear that the F-helix acts as a potential inhibitor to this interaction by physically blocking its path (Figure 1B) (*11*). To investigate the effects of the mutations on polymerization, we used conditions (60 °C) under which all the variants readily polymerized over a reasonable time period (1 h), allowing for a more accurate and reproducible assessment of the aggregation kinetics. Polymers formed through this treatment have been shown to be identical to those observed both in vivo and at lower temperatures (*11*, *36*).

The polymerization characteristics of the proteins were followed using native-PAGE analysis, which tracks the loss of monomeric protein as the protein polymerizes and ultimately is unable to enter the running gel. In addition, the kinetics of the reaction was determined by following the changes in bis-ANS fluorescence as the protein polymerizes. These spectroscopic changes monitor both the rates of conformational change (k_{cc}) and polymerization (k_{agg}) (*25*, *34*). In the absence of mutation, monomeric α_1-AT is not visible by native-PAGE after 30 min of incubation at 60 °C (Figure 3). The kinetics demonstrate that the conformational change from M to M* occurs rapidly ($k_{cc} = 0.025\ s^{-1}$) and that polymers then form with an observed aggregation rate of $4 \pm 0.1 \times 10^{-4}\ s^{-1}$ (Table 2). In contrast, the presence of mutations at positions 149 and 157 accelerate the overall rate of polymerization. Native-PAGE analysis shows that monomeric protein disappeared from the gel within 5 min of incubation. Spectroscopic determination of the kinetic parameters for the reaction demonstrates that both k_{cc} and k_{agg} are significantly faster than that of α_1-AT (Figure 3 and Table 2). Intriguingly, mutation of V161 did not affect the overall rate of polymerization as compared to α_1-AT, as determined by native-PAGE. Kinetic analysis showed that V161I and V161L had unchanged rates of conformational change and aggregation. V161A displayed a 4.4-fold faster rate of conformational change as compared to α_1-AT; however, the rate of aggregation was almost unchanged (Table 2). Cumulatively, these data indicate that the interactions formed between D149 and I157 and other parts of the F-helix and A β-sheet are involved in forming and stabilizing M*. The loss of the hydrophobic interactions between V161 and the underlying A β-sheet showed no effect on the actual polymerization rate (k_{agg}), suggesting that these interactions are absent in M*. Overall, this is indicative of the C-terminal region undergoing a large conformational change during the conversion of M to M* (Figure 4).

Differing Roles of the F-Helix

The ability of a serpin to inhibit proteinases and to polymerize involves similar conformational changes. During both these events, the A β-sheet must open, which allows insertion of either its own RCL (proteinase inhibition) or the RCL from another molecule (polymerization). Our data suggest that the F-helix, which sterically blocks both transitions, responds differently in these scenarios.

Theoretical studies have suggested that the F-helix must undergo reversible conformational changes and that these provide a potential mechanism that makes proteinase inhibition energetically favorable (*12*). Previously, it has been shown that the F-helix is conformationally labile and undergoes a partial unfolding when the A β-sheet expands (*17*). Here, we show that the partial unfolding during proteinase inhibition is limited to both the N- and the C-termini of the helix (Figure 4). While we cannot define these conformational changes at a molecular level, we hypothesize that extending the helix in such a way would allow the helix and the loop connecting the helix to the A β-sheet to become more mobile, which would facilitate the rapid insertions of the RCL during proteinase inhibition. Our data also demonstrate that I157 maintains its interactions throughout the inhibitory pathway and that the loss of these results in increased substrate behavior. Similar behavior was observed in the Rouen IV mutation of antithrombin where loss of N187, which is positioned in the middle of the F-helix, forming critical interactions with strand 3A results in a loss of inhibitory activity (*37*). The requirement for a productive conformational change within the F-helix was also demonstrated when the F-helix in PAI-1 was deleted, which leads to substrate-like behavior in the serpin (*38*).

Serpin polymerization involves a similar conformational change to proteinase inhibition, in that the A β-sheet must expand and RCL residues from another serpin must bury under the F-helix (Figure 1B). Our data demonstrate that polymerization involves the deformation of the C-terminal of the F-helix (Figure 4). This conformational state is reminiscent of the δ conformation, in antichymotrypsin, where the C-terminus of the F-helix is unwound and inserted into the A β-sheet. The δ conformation was shown to be highly polymerogenic (*16*). Related to our polymerization finding is the conformation of the F-helix observed in the folding intermediate; here, the F-helix appears totally disrupted (Figure 4). We propose that the A β-sheet is closed in the folding intermediate conformation, to minimize polymerization, and that the final stage of folding involves expansion of the A β-sheet (*39*) and formation of the F-helix.

Our data and that of others (*12*) indicates that the F-helix is by no means a passive structural element. Here, we have shown that it is able to undergo conformational changes in response to different environmental pressures. So while numerous structures/snapshots of serpin structures have been determined, what is becoming more apparent is that there is an intrinsic complexity in how these conformational changes are achieved, a complexity that undoubtedly gives an evolutionary advantage to the serpin superfamily.

ACKNOWLEDGMENT

We would like to thank Prof. Peter Gettins for his ideas and Judy Lee for her technical assistance.

REFERENCES

1. Carrell, R. W., and Huntington, J. A. (2003) How serpins change their fold for better and for worse, *Biochem. Soc. Symp. 70*, 163−178.
2. Gettins, P. G. (2002) Serpin structure, mechanism, and function, *Chem. Rev. 102*, 4751−804.
3. Huntington, J. A., Read, R. J., and Carrell, R. W. (2000) Structure of a serpin−protease complex shows inhibition by deformation, *Nature 407*, 923−926.
4. Stratikos, E., and Gettins, P. G. (1999) Formation of the covalent serpin−proteinase complex involves translocation of the proteinase by more than 70 Å and full insertion of the reactive center loop into β-sheet A, *Proc. Natl. Acad. Sci. U.S.A. 96*, 4808−4813.

5. Stein, P. E., and Carrell, R. W. (1995) What do dysfunctional serpins tell us about molecular mobility and disease? *Nat. Struct. Biol. 2*, 96−113.
6. Chow, M. K., Lomas, D. A., and Bottomley, S. P. (2004) Promiscuous β-strand interactions and the conformational diseases, *Curr. Med. Chem. 11*, 491−499.
7. Elliott, P. R., Abrahams, J. P., and Lomas, D. A. (1998) Wild-type _1-antitrypsin is in the canonical inhibitory conformation, *J. Mol. Biol. 275*, 419−425.
8. Carrell, R. W., and Owen, M. C. (1985) Plakalbumin, _1-antitrypsin, antithrombin, and the mechanism of inflammatory thrombosis, *Nature 317*, 730−732.
9. Cabrita, L. D., and Bottomley, S. P. (2004) How do proteins avoid becoming too stable? Biophysical studies into metastable proteins, *Eur. Biophys. J. 33*, 83−88.
10. Lomas, D. A., and Carrell, R. W. (2002) Serpinopathies and the conformational dementias, *Nat. Rev. Genet. 3*, 759−768.
11. Sivasothy, P., Dafforn, T. R., Gettins, P. G., and Lomas, D. A. (2000) Pathogenic _1-antitrypsin polymers are formed by reactive loop-β-sheet A linkage, *J. Biol. Chem. 275*, 33663−33668.
12. Gettins, P. G. (2002) The F-helix of serpins plays an essential, active role in the proteinase inhibition mechanism, *FEBS Lett. 523*, 2−6.
13. Stein, P., and Chothia, C. (1991) Serpin tertiary structure transformation, *J. Mol. Biol. 221*, 615−621.
14. Wright, H. T., and Scarsdale, J. N. (1995) Structural basis for serpin inhibitor activity, *Proteins 22*, 210−225.
15. Whisstock, J. C., Skinner, R., Carrell, R. W., and Lesk, A. M. (2000) Conformational Changes in Serpins: I. The Native and Cleaved Conformations of _(1)-Antitrypsin, *J. Mol. Biol. 295*, 651−665.
16. Gooptu, B., Hazes, B., Chang, W. S., Dafforn, T. R., Carrell, R. W., Read, R. J., and Lomas, D. A. (2000) Inactive conformation of the serpin _(1)-antichymotrypsin indicates two-stage insertion of the reactive loop: Implications for inhibitory function and conformational disease, *Proc. Natl. Acad. Sci. U.S.A. 97*, 67−72.
17. Cabrita, L. D., Whisstock, J. C., and Bottomley, S. P. (2002) Probing the Role of the F-Helix in Serpin Stability through a Single Tryptophan Substitution, *Biochemistry 41*, 4575−4581.
18. Picard, V., Marque, P. E., Paolucci, F., Aiach, M., and Le Bonniec, B. F. (1999) Topology of the stable serpin−protease complexes revealed by an autoantibody that fails to react with the monomeric conformers of antithrombin, *J. Biol. Chem. 274*, 4586−4593.
19. Bijnens, A. P., Gils, A., Knockaert, I., Stassen, J. M., and Declerck, P. J. (2000) Importance of the hinge region between _-helix F and the main part of serpins, based upon identification of the epitope of plasminogen activator inhibitor type 1 neutralizing antibodies, *J. Biol. Chem. 275*, 6375−6380.
20. Irving, J. A., Pike, R. N., Lesk, A. M., and Whisstock, J. C. (2000) Phylogeny of the serpin superfamily: Implications of patterns of amino acid conservation for structure and function, *Genome Res. 10*, 1841−1860.
21. Gilis, D., McLennan, H. R., Dehouck, Y., Cabrita, L. D., Rooman, M., and Bottomley, S. P. (2003) In vitro and in silico design of _1-antitrypsin mutants with different conformational stabilities, *J. Mol. Biol.* 325, 581−589.
22. Le Bonniec, B. F., Guinto, E. R., and Stone, S. R. (1995) Identification of thrombin residues that modulate its interactions with antithrombin III and _1-antitrypsin, *Biochemistry 34*, 12241−12248.
23. Dafforn, T. R., Pike, R. N., and Bottomley, S. P. (2004) Physical characterization of serpin conformations, *Methods 32*, 150−158.
24. Pace, C. N. (1986) Determination and analysis of urea and guanidine hydrochloride denaturation curves, *Methods Enzymol. 131*, 266−280.
25. James, E. L., and Bottomley, S. P. (1998) The mechanism of _1-antitrypsin polymerization probed by fluorescence spectroscopy, *Arch. Biochem. Biophys. 356*, 296−300.
26. Hood, D. B., Huntington, J. A., and Gettins, P. G. (1994) _1-proteinase inhibitor variant T345R. Influence of P14 residue on substrate and inhibitory pathways, *Biochemistry 33*, 8538−8547.
27. Chaillan-Huntington, C. E., and Patston, P. A. (1998) Influence of the P5 residue on _1-proteinase inhibitor mechanism, *J. Biol. Chem. 273*, 4569−4573.
28. Pearce, M. C., Rubin, H., and Bottomley, S. P. (2000) Conformational Change and Intermediates in the Unfolding of _1-Antichymotrypsin, *J. Biol. Chem. 275*, 28513−28518.
29. James, E. L., Whisstock, J. C., Gore, M. G., and Bottomley, S. P. (1999) Probing the unfolding pathway of antitrypsin, *J. Biol. Chem. 274*, 9482−9488.
30. Powell, L. M., and Pain, R. H. (1992) Effects of glycosylation on the folding and stability of human, recombinant, and cleaved _1-antitrypsin, *J. Mol. Biol. 224*, 241−252.
31. Yu, M. H., Lee, K. N., and Kim, J. (1995) The Z-type variation of human _1-antitrypsin causes a protein folding defect, *Nat. Struct. Biol. 2*, 363−367.
32. Irun, M. P., Garcia-Mira, M. M., Sanchez-Ruiz, J. M., and Sancho, J. (2001) Native hydrogen bonds in a molten globule: the apoflavodoxin thermal intermediate, *J. Mol. Biol. 306*, 877−888.
33. Yan, S., Gawlak, G., Smith, J., Silver, L., Koide, A., and Koide, S. (2004) Conformational heterogeneity of an equilibrium folding intermediate quantified and mapped by scanning mutagenesis, *J. Mol. Biol. 338*, 811−825.
34. Dafforn, T. R., Mahadeva, R., Elliott, P. R., Sivasothy, P., and Lomas, D. A. (1999) A kinetic mechanism for the polymerization of _1-antitrypsin, *J. Biol. Chem. 274*, 9548−9555.
35. Devlin, G. L., Parfrey, H., Tew, D. J., Lomas, D. A., and Bottomley, S. P. (2001) Prevention of polymerization of M and Z _1-Antitrypsin (_1-AT) with trimethylamine *N*-oxide. Implications for the treatment of _1-at deficiency, *Am. J. Respir. Cell Mol. Biol. 24*, 727−732.
36. Chang, W. S. W., Whisstock, J., Hopkins, P. C. R., Lesk, A. M., Carrell, R. W., and Wardell, M. R. (1997) Importance of the Release of Strand 1c to the Polymerization Mechanism of Inhibitory Serpins, *Protein Sci. 6*, 89−98.
37. Bruce, D., Perry, D. J., Borg, J. Y., Carrell, R. W., and Wardell, M. R. (1994) Thromboembolic disease due to thermolabile conformational changes of antithrombin Rouen-VI (187 Asn → Asp), *J. Clin. Invest. 94*, 2265−2274 [see comments].
38. Vleugels, N., Gils, A., Bijnens, A., Knockaert, I., and Declerck, P. J. (2000) The importance of helix F in plasminogen activator inhibitor-1, *Biochim. Biophys. Acta 1476*, 20−26.
39. Tew, D. J., and Bottomley, S. P. (2001) Probing the equilibrium denaturation of the serpin _1-Antitrypsin with single tryptophan mutants; evidence for structure in the urea unfolded state, *J. Mol. Biol. 313*, 1163−1171.

BI0491346